Gao *et al.*
Journal of Orthopaedic Surgery and Research (2025) 20:441
https://doi.org/10.1186/s13018-025-05804-1

Journal of Orthopaedic Surgery and Research

RESEARCH

Open Access

Obacunone acts as a histone deacetylase 1 inhibitor to limit p38MAPK signaling and alleviate osteoarthritis progression

Yong Gao[1], Ke Wang[2], Chao Shi[1], Yang Gao[1] and De-Qian Kong[1*]

Abstract

Background Osteoarthritis (OA) is an age-related progressive degenerative disorder characterized by cartilage extracellular matrix degradation and inflammation. In this study, we explored the function and mechanism of action of obacunone (OB) in inhibiting OA progression.

Methods The degradation of articular cartilage and its severity were examined using Safranin O-fast green and hematoxylin and eosin (HE) staining. Chondrocyte survival was evaluated using a cell counting kit-8 assay. In addition, qRT-PCR, western blot analysis, immunohistochemical staining, and enzyme-linked immunosorbent assay were performed to evaluate the effects of OB on cartilage injury.

Results OB mitigated cartilage lesions in rats with anterior cruciate ligament transaction-induced OA. The protein expression of collagen II was increased and the protein expression of ADAM metallopeptidase with thrombospondin type 1 motif 5 (ADAMTS-5), matrix metalloproteinase (MMP)-13, and RUNX family transcription factor 2 (RUNX2) was reduced in the articular cartilage of OB-treated rats. Moreover, OB exhibited anti-inflammatory activities by reducing the serum levels of interleukin (IL)-6, tumor necrosis factor (TNF)-α, IL-1β, and IL-18. In IL-1β-stimulated primary chondrocytes, OB dose-dependently elevated the expression of collagen II, and decreased the expression of ADAMTS-5, MMP-13, RUNX2 and inflammatory cytokines. Histone deacetylase 1 (HDAC1) was identified as a predicted OB target. OB inhibited HDAC1 expression to limit the activation of p38MAPK signaling. The transfection of chondrocytes with HDAC1 or p38MAPK overexpression plasmids reversed the chondroprotective effects of OB.

Conclusion OB mitigated OA progression by binding to HDAC1 and inhibiting p38MAPK signaling, indicating that OB may be a promising drug for the treatment of OA.

Highlights

1. Obacunone mitigates cartilage lesions in rat with ACLT-induced OA;
2. Obacunone inhibits cartilage ECM degradation and inflammation in rats;
3. Obacunone protects primary chondrocytes against IL-1β-induced damage;
4. Obacunone acts as a HDAC1 inhibitor to limit the activation of p38MAPK signaling.

Keywords Osteoarthritis, Obacunone, HDAC1, p38MAPK signaling

*Correspondence:
De-Qian Kong
deqian86@163.com
Full list of author information is available at the end of the article

Introduction

Osteoarthritis (OA) is a well-known degenerative joint disease and a leading cause of disability affecting 7.6% of people worldwide [1, 2]. Its prevalence is continuously increasing owing to current unhealthy lifestyles and aging populations. Moreover, OA is more prevalent in women than in men [3]. OA typically affects the knees, spine, hands, and hips. The primary hallmarks of OA include articular cartilage degradation, severe synovitis, osteophyte development, and subchondral bone thickening [4]. Investigations of the complex crosstalk among various joint tissues and increasing evidence have demonstrated that OA is a chronic inflammatory disorder involving an imbalance in inflammation-associated cytokines [5, 6]. According to previous reports, type II collagen, aggrecan, matrix metalloproteinases (MMPs), and ADAM metallopeptidase with thrombospondin type 1 motif 5 (ADAMTS-5) contribute to the development of OA [7]. Drugs that regulate degradation-related proteins and inflammatory cytokines have been considered important candidates for OA treatment [8, 9].

Obacunone (OB) is a natural triterpenoid widely found in citrus species and Rutaceae family members, like *Phellodendri Cortex* [10]. *Phellodendri Cortex* is the monarch herb in Si-Miao-Wan (SMW) formula, which has been widely used in the clinic of China for treating arthritis [11]. In addition, He et al. [12] and Hu et al. [13] demonstrated that OB suppresses osteoclast formation and attenuates ovariectomy-induced bone loss. Park et al. [14] reported that OB promotes osteoblast differentiation and bone mineralization. These findings highlight OB as a potential therapeutic candidate for arthritis and osteoporosis.

In this study, a rat model of OA was established to evaluate the therapeutic potential of OB by assessing cartilage lesions, enzyme degradation, and inflammation. The effects of OB on primary chondrocytes treated with interleukin (IL)-1β were also measured. The mechanism of action of OB in protecting primary chondrocytes was preliminarily elucidated. The findings of this study may lay the groundwork for future investigations on OA treatment.

Methods

Anterior cruciate ligament transaction (ACLT) model

This study was approved by the Ethics Committee of the Affiliated Hospital of the Second Affiliated Hospital of Shandong First Medical University. Animal experiments were performed in accordance with the ARRIVE guidelines. Thirty Sprague–Dawley (SD) rats (male, 8-weeks old) were purchased from Jinan Pengyue Experimental Animal Breeding Co., Ltd. (Jinan, China) and bred under specific pathogen-free conditions with a 12 h/12 h dark/light cycle for 7 days. Rats were randomly divided into five groups (six rats per group): Sham, ACLT, ACLT + OB (2.5 mg/kg), ACLT + OB (5 mg/kg), and ACLT + OB (10 mg/kg). OB (purity 99.75%), cycloheximide (CHX), and IL-1β were purchased from MedChemExpress (Monmouth Junction, NJ, USA). For ACLT, the rats were anesthetized with an intraperitoneal injection of 40 mg/kg pentobarbital sodium. The right hind limb of each rat was prepared and disinfected, and a longitudinal incision of approximately 3 cm was made inside the knee joint. A small incision was made along the patellar ligament, the muscles were cut, the knee was bent, and the patella was everted. After exposing the cruciate ligament, the anterior cruciate ligament was cut. A drawer test was performed to confirm whether the anterior cruciate ligament was completely severed, and the wound was sutured layer-by-layer [15]. The rats in the sham group underwent arthrotomy without transection of the anterior cruciate ligament in the right hind limb. Following ACLT surgery, the rats were intraperitoneally injected with 2.5, 5, or 10 mg/kg OB daily for 6 weeks. OB was dissolved in DMSO and diluted with saline to a final DMSO concentration of less than 0.1%. Finally, all rats were sacrificed after anesthesia with an intraperitoneal injection of 40 mg/kg pentobarbital sodium. The femurs of rats were collected, fixed in formalin, decalcified using EDTA (0.5 M, pH 8.0) for 4 weeks, dehydrated, and embedded in paraffin. Rat blood samples were collected from the tail vein six weeks after OB administration commenced. The concentration of cartilage oligomeric matrix protein (COMP) in the supernatant of serum was measured using an enzyme-linked immunosorbent assay (ELISA) kit (Elabscience, Wuhan, China).

Safranin O-fast green and hematoxylin and eosin (HE) staining

Tissue samples were sliced to 4 μm thickness and stained using a Safranin O and Fast Green Cartilage staining kit (Beyotime, Shanghai, China) or HE staining kit (Sangon Biotech, Shanghai, China). Histopathological changes were observed under a light microscope. The Osteoarthritis Research Society International (OARSI) scoring method [16] was used to assess the articular cartilage degeneration, where 0 = normal, 1 = small fibrillations without loss of cartilage, 2 = low degeneration (vertical clefts down to the layer immediately below the superficial layer and some loos of surface lamina), 3 = mild degeneration (vertical clefts/erosion to the calcified cartilage extending to < 25%), 4 = moderate degeneration (25–50%), 5 = marked degeneration (50–75%), and 6 = severe degeneration (> 75%). This process was completed by two blinded researchers and the average score was used to reduce observer bias.

Immunohistochemical (IHC) study

Decapitate the bone tissue with EDTA, then dehydrate it with a gradient of alcohol in the dehydrator. After soaking and embedding the bone tissue in wax, the wax block was placed in a paraffin slicer and sliced into 4 μ m slides. After dewaxing and rehydration, tissue sections were boiled in 0.01 M citric acid (pH 6.0) for 10 min for antigen retrieval. Sections were maintained in 3% H_2O_2 for 30 min and subjected to goat serum blockade. These slides were incubated with a primary antibody against collagen II (ab34712; Abcam, Cambridge, MA) at 4 °C overnight, washed twice in phosphate-buffered saline (PBS) and blocked with a secondary antibody (ab6721; Abcam) at 37 °C for 1 h. To indicate the location of the target antigen, the slides were incubated with 3, 3′-diamino-benzidine (DAB, BOSTER Biological Technology, Wuhan, China). The signals were photographed under a light microscope (Leica DM4000 B; Leica Microsystems Inc., Germany).

Primary rat chondrocyte isolation and culture

Rat chondrocytes were isolated from the cartilage tissues of healthy rats. The fresh cartilage was minced and digested in 0.25% trypsin for 20 min and maintained in 0.2% collagenase II for 6 h at 37 °C with 5% CO_2. Subsequently, the suspension was centrifuged at 1000 r/min for 5 min. The chondrocytes were incubated in DMEM-F12 culture medium (Invitrogen, Carlsbad, CA, USA) containing 10% fetal bovine serum (FBS) and 1% penicillin/streptomycin at room temperature with 5% CO_2. OB was dissolved in DMSO and diluted with the culture medium to obtain the final treatment concentrations of OB. Rat chondrocytes were treated with 20, 40, or 80 μM OB for 48 h with or without the treatment of 10 ng/mL IL-1β.

Cell transfection

Chondrocytes were seeded in 24-well plates at a density of 2×10^4 cells/well, and cell transfection was performed until cell confluence reached 60–70%. Based on the manufacturer's instructions, chondrocytes were transfected with 1 μg/well histone deacetylase 1 (HDAC1) (NM_001025409.1) or p38MAPK (NM_031020.3) overexpression plasmids using lipofectamine 3000 (Invitrogen) at 37 °C with 5% CO_2 for 48 h. An empty pcDNA3.1 vector was transfected as an overexpression negative control (OE-NC). For siRNA transfection, the following siRNAs were used: si-HDAC1 #1 (5'-GGCACCAAG AGGAAAGTCTGT-3'), si-HDAC1 #2 (5'-GCACCA AGAGGAAAGTCTGTT-3'), and siNC (5'-GCGATG AACCGCGAAGTGATA-3').

Cell counting kit 8 (CCK-8) assay

Primary rat chondrocytes in the logarithmic growth phase were seeded in 96-well plates at a density of 5×10^3 cells/well. Following OB treatment (20, 40, or 80 μM) for 48 h, cells were treated with 10 μL CCK-8 reagent (Beyotime) at 37 °C for 1.5 h. Absorbance was measured using a microplate reader (Bio-Rad Laboratories, Hercules, CA, USA).

Flow cytometry

Following OB treatment (20, 40, or 80 μM) for 48 h, primary rat chondrocytes were collected using 0.25% trypsin solution without EDTA (Beyotime). A sample of 1×10^5 cells was added to Annexin V-FITC binding buffer, stained with 5 μL Annexin V-FITC and 10 μL PI (Beyotime), and incubated at room temperature for 20 min in darkness. Apoptotic cells were analyzed using flow cytometry (BD Biosciences, Franklin Lakes, NJ, USA) and counted using FlowJo software (Tree Star, Inc.).

qRT-PCR

Total RNA extracted from cells and tissues using Trizol purification was denatured at 95 °C for 5 min. For the rat cartilage tissues, a thin layer of cartilage was detached from adult rats using microforceps and microscissors. The isolated RNA (500 ng) was transcribed into cDNA using a RevertAid First Strand cDNA Synthesis Kit (Thermo Fisher Scientific, Waltham, MA, USA). Quantitative real-time PCR (qPCR) was performed using SYBR Green Mastermix (KAPA Biosystems, Woburn, MA, USA) on an ABI7500 Real-Time PCR System (Applied Biosystems, Foster City, CA, USA). Reaction conditions were as follows: Pre denaturation 95 °C for 30 s, amplification 95 °C for 10 s, 65 °C for 45 s (40 cycles) and 72 °C for 2 min. β-actin served as an internal reference, and target gene expression was normalized to β-actin using the $2^{-\Delta\Delta Ct}$ method. The following primer sequences were used: *Col2a1*, 5'-ATGTATGGAAGCCCTCGT CC-3' (forward), 5'- TGGCCCTAATTTTCCACTGGC-3' (reverse); *Adamts5*, 5'- ATGCACTTCAGCCACGAT CA-3' (forward), 5'-TCCATGGCTTGATGTCGAGT-3' (reverse); *Mmp13*, 5'-GACAAGCAGCTCCAAAGG CTA-3' (forward), 3'-CAGTTCAGGCTCAACCTG CT-5' (reverse); *Runx2*, 5'-CAAGGAGGCCCTGGTGTT TA-3' (forward), 5'-TTGCAGCCTTAAATGACTCGG-3' (reverse); and *β-actin*, 5'-CCCGCGAGTA CAACCT TCTTG-3' (forward), 5'-GTCATCCATGGCGAACTG GTG-3' (reverse).

Western blotting

Proteins were extracted from cartilage tissues and cells using RIPA lysis buffer (Beyotime). Protein sample (20 μg per lane) was separated using 10% SDS-PAGE and then transferred onto polyvinylidene fluoride (PVDF) membrane. PVDF membranes were blocked in 5% skimmed milk at 25 °C for 2 h and sealed with primary antibodies, including collagen II (ab34712; Abcam), ADAMTS-5 (ab231595; Abcam), MMP13 (SAB4501900; Sigma-Aldrich, St. Louis, MO), RUNX2 (ab114133; Abcam), and actin (20,536–1-AP; Proteintech, Wuhan, China) at 4 °C overnight. After washing twice with PBS for 5 min, PVDF membranes were incubated with a secondary antibody (ab205718; Abcam) at 25 °C for 2 h. The protein band signals were developed using the High-Sensitive Plus ECL luminescence reagent (Sangon Biotech).

ELISA

The serum and cell culture supernatant were isolated and stored at -80 °C for subsequent use for measuring inflammatory cytokine levels using IL-6 (E-EL-R0015; Elabscience), TNF-α (CSB-E11987r-IS; Cusabio, Wuhan, China), IL-1β (E-EL-R0012; Elabscience), and IL-18 (CSB-E04610r; Cusabio) ELISA kits. Optical density (OD) was determined at 450 nm using a microplate reader (Bio-Rad).

Bioinformatic analysis

The SwissTargetPrediction (http://www.swisstargetprediction.ch/) and Prediction (https://prediction.charite.de/subpages/target_prediction.php) databases were used to identify potential OB targets. The OA targets were identified using the GeneCards database (https://www.genecards.org/). The relevance scores for these targets were calculated and targets with relevance scores equal to or above the median were selected as potential candidates for further analysis. A Venn diagram was created using Venny 2.1.0. The protein–protein interaction (PPI) network for hub genes was constructed using the cytoHubba plugin in Cytoscape 3.10.0. The interaction score was set at the highest confidence (≥ 0.9000) as the threshold. The CytoHubba plugin of Cytoscape3.10.0 was used to screen hub genes using the MCC algorithm. Gene Ontology (GO) and Kyoto Encyclopedia of Genes and Genomes (KEGG) were used for the pathway enrichment analysis. Molecular docking between OB and its targets was performed in a Molecular Operating Environment (MOE).

Statistical analysis

Data are presented as mean ± standard deviation (SD). GraphPad Prism software 8.0 version (GraphPad Software, Inc., La Jolla, CA, USA) were used to analyze the data. Statistical analyses were performed with one-way ANOVA followed by Tukey's post hoc test or two-way ANOVA followed by Bonferroni's post hoc test. Statistical significance was set at 0.05.

Results

OB ameliorates cartilage lesions in rat with ACLT-induced OA

To determine the effect of OB on OA progression, rat ACLT models were established and administered 2.5, 5, or 10 mg/kg OB. Safranin O-fast green and HE staining were performed to evaluate the structural integrity of the articular cartilage. Compared with sham rats, the joint tissues in ACLT rats were significantly degenerated and damaged, as evidenced by the loss of Safranin O staining, abnormal cellular morphology, and layering with an abnormal tidal line (Fig. 1A). Administration of OB alleviated the degeneration and damage to joint tissues following ACLT. The OARSI score was significantly higher in the ACLT model group than in the sham operation group, whereas OB treatment lowered the scores in a dose-dependent manner (Fig. 1B). In addition, the COMP levels in rat serum were elevated by ACLT and reduced by OB administration in a dose-dependent manner (Fig. 1C). These data demonstrated the functional effects of OB on the amelioration of cartilage lesions in ACLT rats.

OB regulates degradation enzymes and inflammation in rat with ACLT-induced OA

To further investigate the role of OB in OA development, the expression of collagen II was measured. IHC results showed that the staining intensity of collagen II was lower in the ACLT group than in the sham group (Fig. 2A). OB administration alleviated the inhibitory effects of ACLT on collagen II expression in a dose-dependent manner. qRT-PCR data showed that, compared with the sham group, ACLT decreased the expression of *Col2a1* and increased the levels of *Adamts5*, *Mmp13*, and *Runx2* (Fig. 2B). OB treatment dose-dependently increased the expression of *Col2a1* and decreased the levels of *Adamts5*, *Mmp13*, and *Runx2*. In addition, ELISA assay results revealed that the levels of inflammatory cytokines, including IL-6, TNF-α, IL-1β, and IL-18, in the serum of ACLT-treated rats were significantly increased compared to those in the sham group (Fig. 2C). However, OB administration remarkably reduced the levels of IL-6, TNF-α, IL-1β, and IL-18 in a dose-dependent manner. These data indicated the effects of OB on the

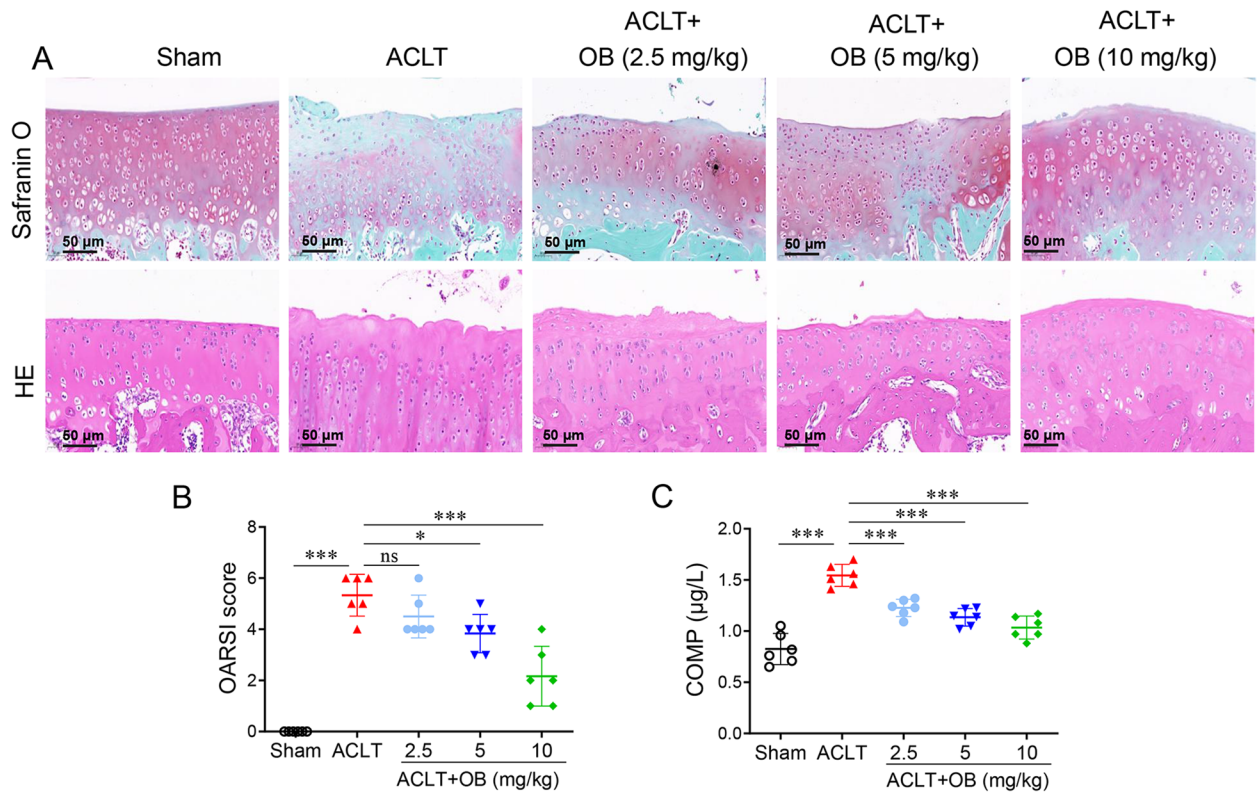

Fig. 1 Obacunone (OB) ameliorates cartilage lesions in rat with ACLT-induced OA. **A** Safranin O-fast green (Top) and HE staining (Bottom) assays were performed to detect the structural integrity of the articular cartilage in ACLT rats administrated with 2.5, 5, or 10 mg/kg OB. Scale bar = 50 μm. **B** OARSI score was used to evaluate the articular cartilage based on the results of Safranin O-fast green staining. **C** The level of COMP in rat serum was measured for the detection of articular cartilage. $n=6$. Data were analyzed by one-way ANOVA followed by Tukey's post hoc test. *$P<0.05$ and ***$P<0.001$

regulation of degradation enzymes and inflammation in ACLT rats.

OB regulates degradation enzyme levels in IL-1β-treated chondrocytes

The functional effects of OB were confirmed in vitro using primary chondrocytes. First, the toxicity of OB on primary chondrocytes was tested using flow cytometry and the CCK-8 assay. Concentrations of OB ranging from 20 to 80 μM showed no toxicity in primary chondrocytes, as no changes in apoptosis and survival were observed (Fig. 3A, B). Primary chondrocytes were treated with IL-1β to mimic the cartilage injury in OA. Cell survival was significantly reduced by IL-1β treatment, whereas OB treatment promoted cell survival in a dose-dependent manner (Fig. 3C). The qRT-PCR and western blotting analyses showed that the expression of collagen II was reduced while the expression of ADAMTS-5, MMP13, and RUNX2 were increased in IL-1β-treated group (Fig. 3D and E). Treatment of cells with OB increased collagen II expression in a dose-dependent manner and reduced ADAMTS-5, MMP13, and RUNX2 expression. These results indicate that OB protects chondrocytes against IL-1β-induced degradation enzyme dysregulation in vitro.

OB inhibits inflammation in IL-1β-treated chondrocytes

To determine the impact of OB on primary chondrocytes following IL-1β treatment, we also evaluated the expression of inflammatory cytokines. As shown in Fig. 4A and B, IL-1β treatment induced significantly higher levels of cytokines, including IL-6, TNF-α, and IL-18. Treatment with OB dose-dependently reduced the levels of these cytokines, showing the anti-inflammatory potential of OB in IL-1β-treated chondrocytes.

OB acts as an inhibitor of HDAC1 to limit p38MAPK signaling

To investigate the underlying mechanism of OB in OA, the targets of OB and OA were screened and intersected. As shown in the Venn diagram, there were 80 potential targets (Fig. 5A), including the HDACs (HDAC1, 2, 3, 4, and 9), which are novel therapeutic targets for OA [17, 18]. Pathway enrichment analysis was then performed

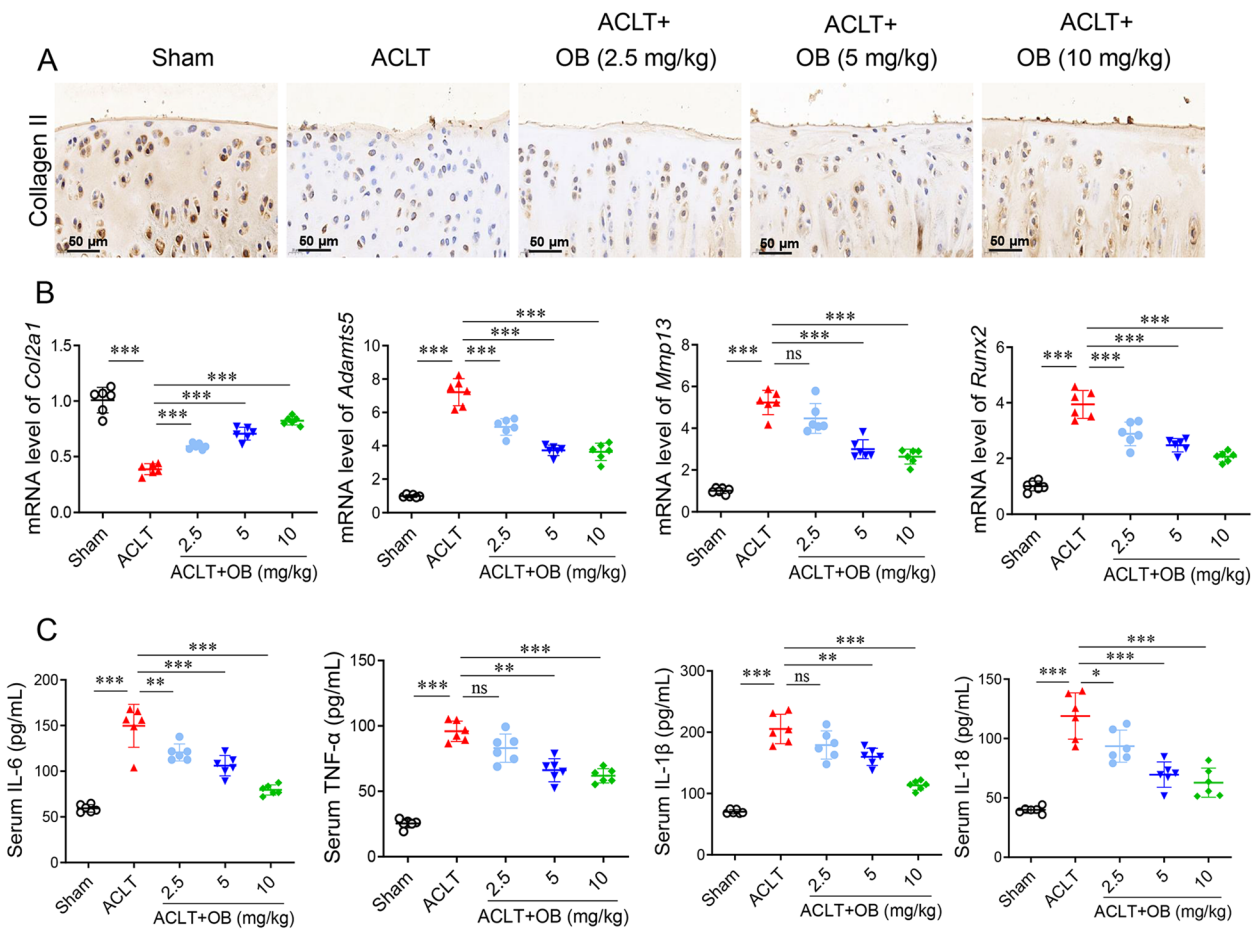

Fig. 2 Obacunone (OB) regulates degradation enzymes and inflammation in rat with ACLT-induced OA. **A** IHC staining for collagen II in articular cartilage of ACLT rats administrated with 2.5, 5, or 10 mg/kg OB. **B** qRT-PCR was employed to quantity the mRNA expression of *Col2a1*, *Adamts5*, *Mmp13*, and *Runx2* in articular cartilage tissues. **C** ELISA analysis was employed to measure the levels of IL-6, TNF-α, IL-1β, and IL-18 in serum. $n=6$. Data were analyzed by one-way ANOVA followed by Tukey's post hoc test. *$P<0.05$, **$P<0.01$ and ***$P<0.001$

using these targets. The GO and KEGG analyses indicated that the molecular functions (MF) of these targets were mainly focused on protein binding and histone deacetylase (HDAC) activity (Fig. 5B). Next, we performed molecular docking between OB and HDACs, including HDAC1, 2, 3, 4, and 9, using the MOE software (Fig. 5C). The docking scores for OB and the HDACs were as follows: HDAC1 (-5.51 kcal/mol), HDAC2 (-5.29 kcal/mol), HDAC3 (-5.91 kcal/mol), HDAC4 (-6.13 kcal/mol), and HDAC9 (-4.77 kcal/mol). These scores indicated that OB has the potential to act as a pan-HDAC inhibitor for inhibiting HDAC1, 2, 3, and 4. In addition, the binding models OB with of HDAC1 and HDAC2 showed H-acceptor and pi-H bond interactions, suggesting that these two have better physical interactions with OB than with the others. We chose HDAC1 for further study as the binding model of HDAC1 has a lower RMSD score than HDAC2 (1.48 Å vs. 4.11 Å), which reflected the reliability of the binding model. The PPI network was constructed using STRING database (Fig. 5D) and visualized using Cytoscape3.10.0 (Fig. 5E). The top ten hub genes, which were highly connected genes in the PPI network, were screened using the Cytoscape plugin cytoHubba. Figure 5F shows that Mapk14 (p38) was one of the top ten hub genes. Considering that it has been widely shown that HDAC inhibitors inhibit p38MAPK signaling to limit OA progression [17], we preliminary inferred that p38MAPK may be the downstream signaling mechanism by which OB inhibits HDACs.

We examined the inhibitory effects of OB on HDAC1 expression. In primary chondrocytes, OB dose-dependently reduced the protein expression of HDAC1 with or without IL-1β stimulation (Fig. 5G). A protein synthesis inhibitor (CHX) was added to evaluate the effect of OB on HDAC1 protein stability. As shown in Fig. 5H,

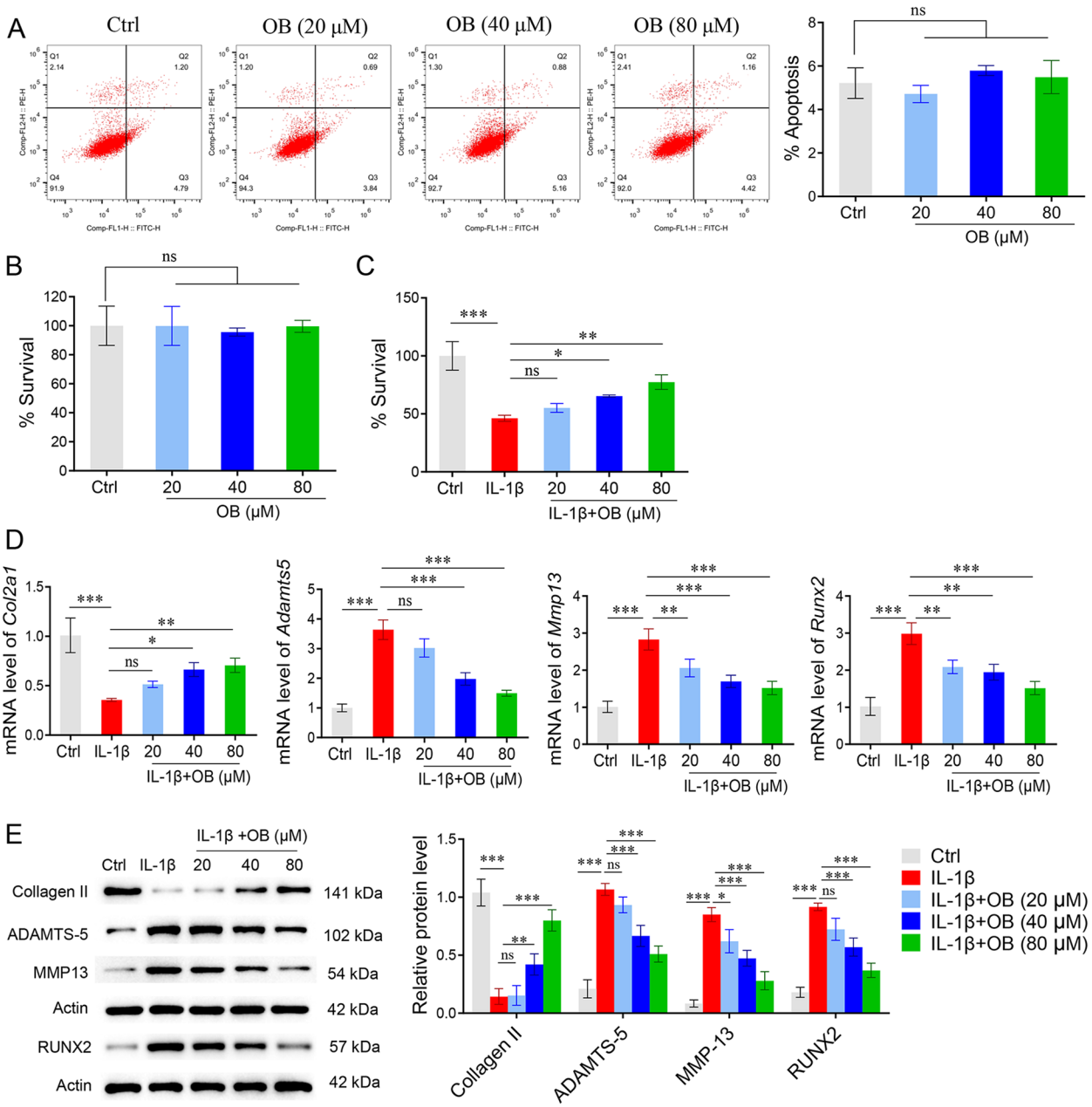

Fig. 3 Obacunone (OB) regulates degradation enzyme levels in IL-1β-treated chondrocytes. The primary chondrocytes were treated with 20, 40, and 80 μM OB. **A** Cell apoptosis and (**B**) survival were respectively detected by flow cytometry and CCK-8 assay. **C** The primary chondrocytes were treated with 20, 40, and 80 μM OB in the presence of IL-1β. CCK-8 assays were performed for detecting cell survival. **D** qRT-PCR was employed to quantity the mRNA expression of *Col2a1*, *Adamts5*, *Mmp13*, and *Runx2* in cell. **D** Western blotting was performed for detecting the protein expression of collagen II, ADAMTS-5, MMP13, and RUNX2. $n = 3$. Data were analyzed by one-way ANOVA followed by Tukey's post hoc test. *$P<0.05$,**$P<0.01$ and ***$P<0.001$

80 μM OB remarkably accelerated the degradation of HDAC1. Western blotting (Fig. 5I) showed that treating cells with OB or transfecting cells with HDAC1 siRNAs remarkably downregulated the expression of phosphorylated p38MAPK. Moreover, HDAC1 overexpression reversed the inhibitory effects of OB on phosphorylated p38MAPK. Taken together, these results indicated that OB could bind to HDAC1 to damage its protein stability and inhibit the activation of p38MAPK in chondrocytes.

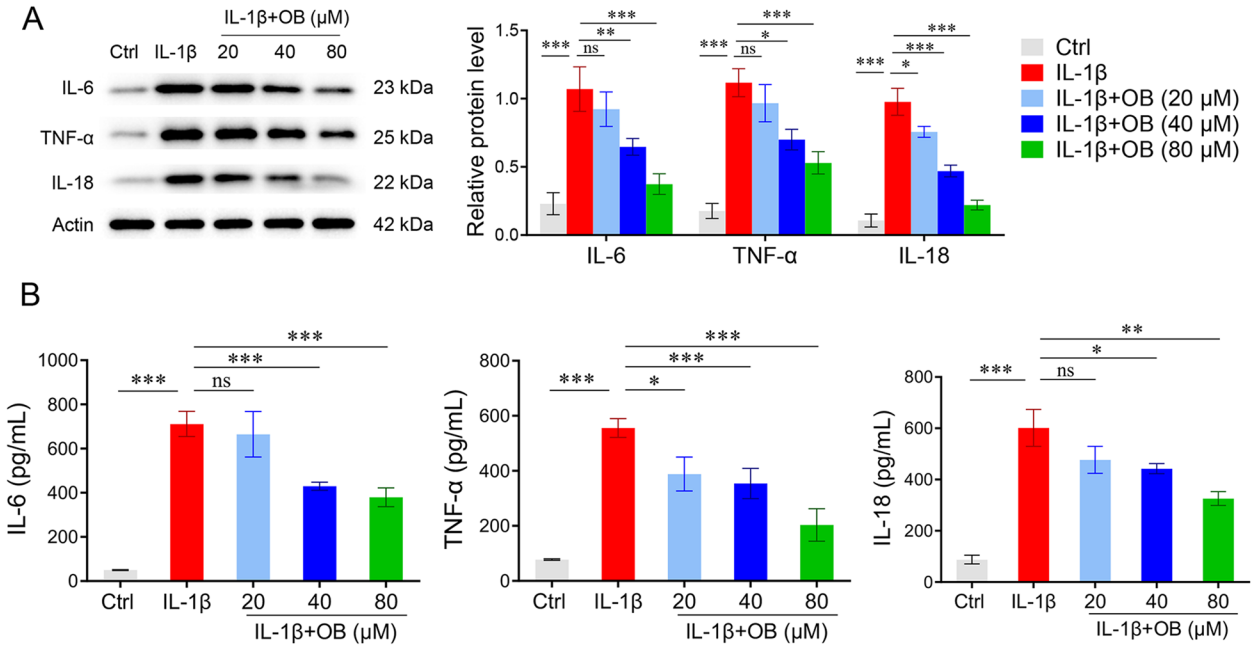

Fig. 4 Obacunone (OB) inhibits inflammation in IL-1β-treated chondrocytes. **A** Western blotting was performed for detecting the protein expression of IL-6, TNF-α, and IL-18. **B** ELISA analysis was employed to measure the levels of IL-6, TNF-α, and IL-18 in the supernatant of primary chondrocytes. $n = 3$. Data were analyzed by one-way ANOVA followed by Tukey's post hoc test. *$P<0.05$, **$P<0.01$ and ***$P<0.001$

Induction of HDAC1 expression or p38MAPK signaling reversed the protective action of OB on chondrocyte damage

To verify the involvement of HDAC1 and p38MAPK in the protective action of OB in chondrocytes, primary chondrocytes were transfected with HDAC1 or p38MAPK overexpression plasmids. Transfection efficiency was verified using western blotting (Fig. 6A). As shown in Fig. 6B, OB treatment significantly elevated cell survival compared with that in the IL-1β-treated group. Compared with OE-NC transfection, HDAC1 or p38MAPK overexpression both significantly reduced cell survival. The expression changes of collagen II, ADAMTS-5, MMP13 and inflammatory cytokines (IL-6, TNF-α, and IL-18) were analyzed using western blotting (Fig. 6C and D). OB treatment significantly increased the expression of collagen II and decreased the expression of ADAMTS-5, MMP13, IL-6, TNF-α, and IL-18. These OB-induced protein changes were reversed by HDAC1 or p38MAPK overexpression. Ultimately, these data revealed that OB mitigates IL-1β-induced chondrocyte damage via inhibition of HDAC1/p38MAPK signaling.

Discussion

OA is an age-associated disease with no current cure [19]. This study demonstrated that the natural triterpenoid OB effectively relieved OA progression in vivo and protected the primary chondrocytes from IL-1β-induced damage. Molecular docking simulations revealed that OB acts as a HDAC1 inhibitor and reduces HDAC1 protein stability. HDAC1 inhibition limits the activation of p38MAPK to control OA progression. These findings suggest that OB is a potential agent for the prevention and treatment of OA.

The extracellular matrix (ECM) of articular cartilage is composed of collagen II and aggrecan, which are responsible for providing tensile strength and elasticity, respectively [20]. During the development of OA, the loss of collagen II and the degradation of aggrecan by MMPs and ADAMTS are recognized as mechanisms of cartilage degradation, which leads to joint pain and disability [20]. For these cartilage ECM, RUNX2 is a critical transcription factor that is highly expressed in human OA cartilage [21]. Recently, natural compounds such as curcumin and oleuropein have been suggested to be effective in preventing cartilage ECM degradation by inhibiting MMP-13, ADAMTS-4, and ADAMTS-5 expression, and inducing collagen II expression [22–24]. In this study, the effects of OB on ameliorating cartilage lesions and cartilage ECM degradation were demonstrated in rats with ACLT-induced OA and in IL-1β-treated primary chondrocytes. Although previous studies have reported the beneficial effects of OB in treating bone diseases, including osteoporosis [12–14], to the best of our knowledge this study is the first to suggest OB as a potential therapeutic agent for the treatment of OA.

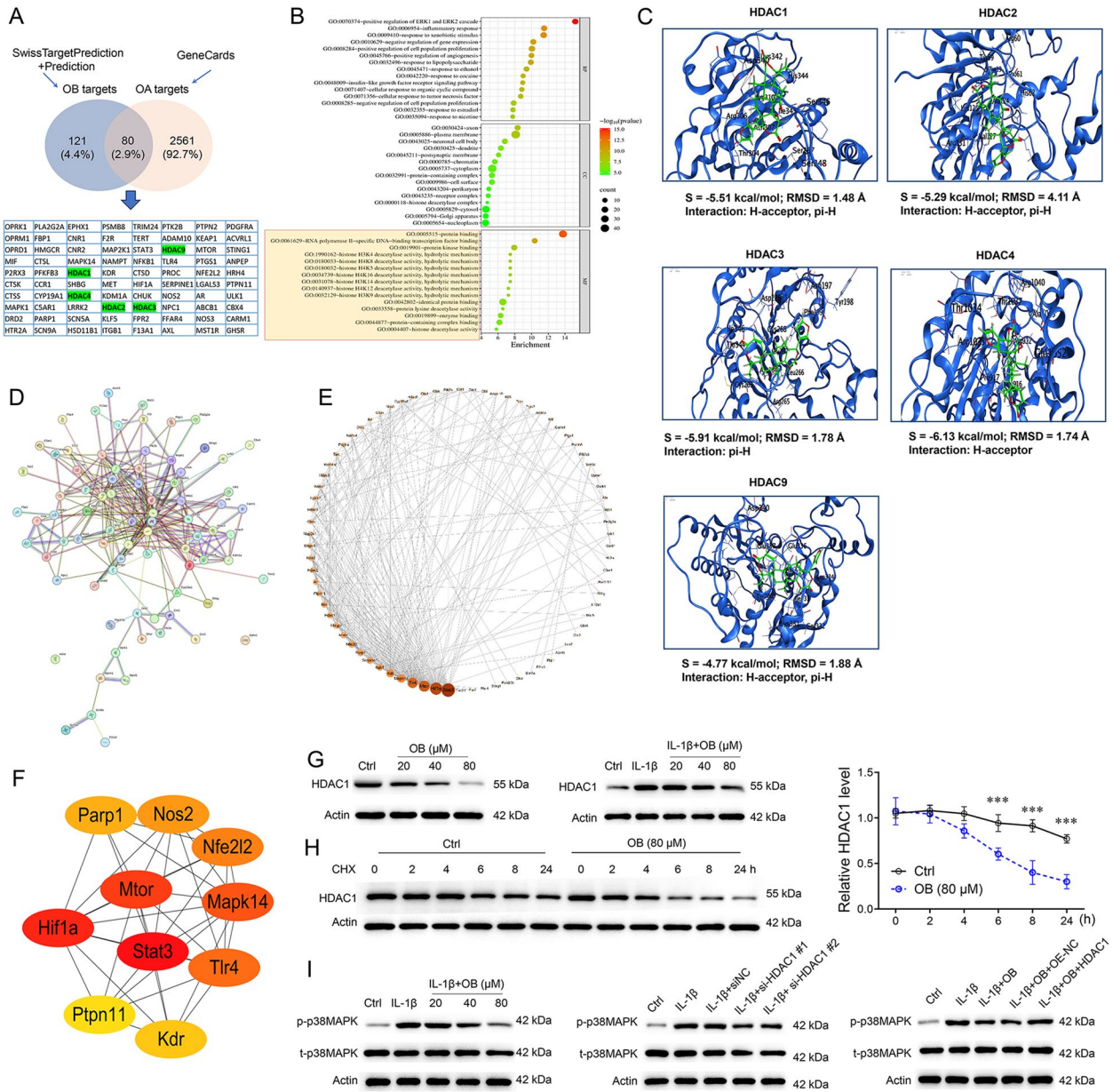

Fig. 5 Obacunone (OB) acts as an inhibitor of HDAC1 to limit p38MAPK signaling.**A** Venn diagram of the targets for OB and OA. **B** GO and KEGG analysis of downstream signaling pathways for OB. **C** The 3D views of molecular docking of OB and its target proteins (HDAC1, 2, 3, 4, and 9) using MOE software. **D** PPI network was made using STRING database and visualized using (**E**) Cytoscape3.10.0. (**F**) The top ten hub genes in PPI network. **G** The primary chondrocytes were treated with 20, 40, and 80 μM OB in the absence and presence of IL-1β. Western blot was performed to detect the protein expression of HDAC1. **H** A protein synthesis inhibitor (CHX) was added to incubate cells for 0~24 h, the protein stability of HDAC1 under OB treatment was analyzed. **I** Western blot was performed to detect the activation of p38MAPK. $n = 3$. Data were analyzed by two-way ANOVA followed by Bonferroni's post hoc test. ***$P<0.001$

In this study, the decreased Runx2 expression was observed following OB treatment. Interestingly, Park et al. [14] observed the upregulated Runx2 in OB-treated osteoblasts. This contradiction might be occurred due to the following reasons. 1) Runx2 is expressed as two isoforms (type-I and type-II) differing only in their amino terminal sequences. The amino terminus of type-I contains MRIPV instead of MASNSLFSAVTPCQQSFFW in type-II. Type-II Runx2 considered to be osteoblast specific. Its function involved in regulation of osteogenic genes (e.g., osteocalcin, osteopontin) to promote osteoblast differentiation [25]. Type I

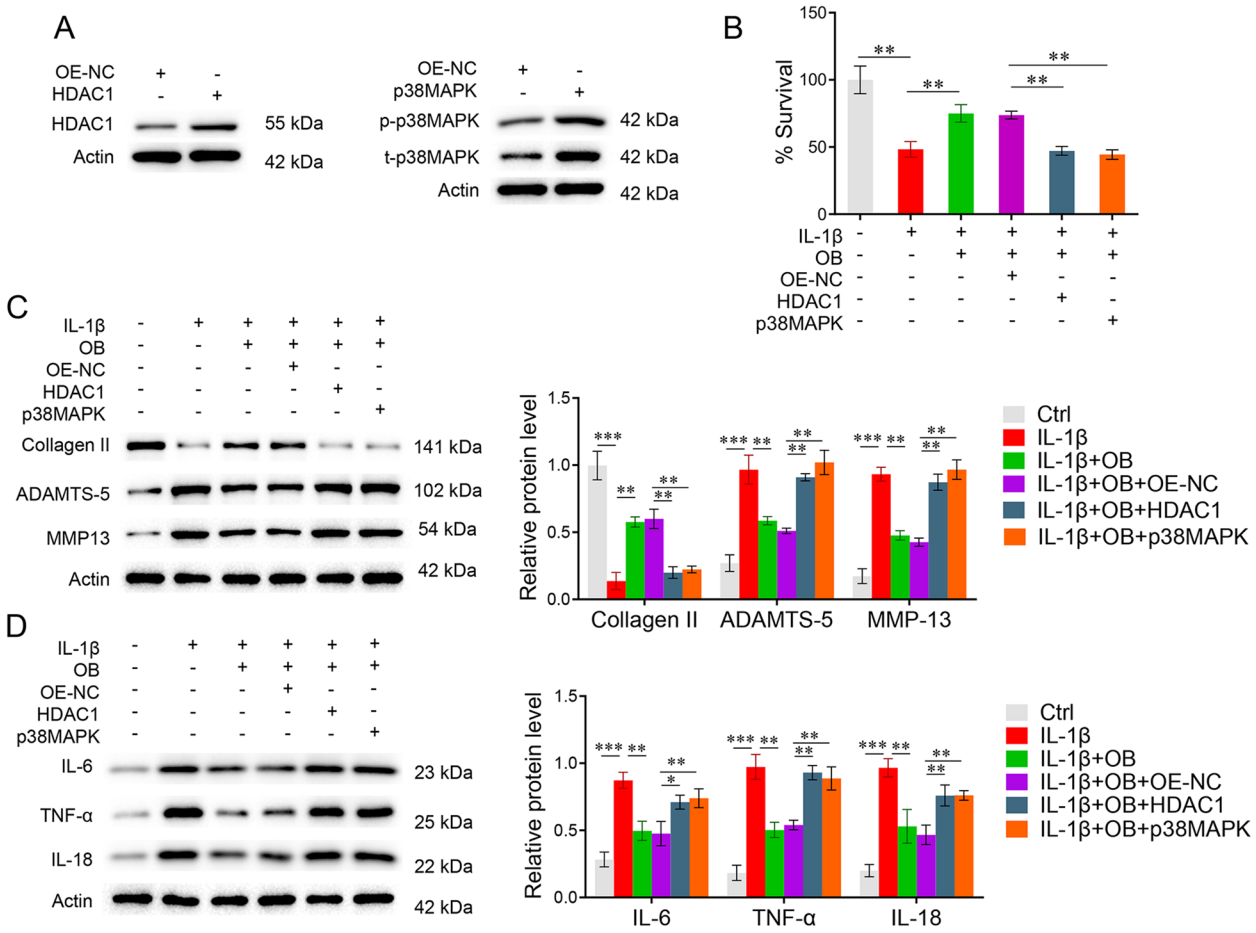

Fig. 6 Induction of HDAC1 expression or p38MAPK signaling reversed the protective action of obacunone (OB) on chondrocyte damage. **A** Primary chondrocytes were transfected with HDAC1 or p38MAPK overexpression plasmids. The transfection efficiency was verified by performing western blotting. **B** Cell survival following transfection and the treatment of IL-1β and OB was detected by CCK-8 assay. **C** Western blotting was performed for detecting the protein expression of collagen II, ADAMTS-5, and MMP13 (**D**) Western blotting was performed for detecting the protein expression of IL-6, TNF-α, and IL-18. $n = 3$. Data were analyzed by one-way ANOVA followed by Tukey's post hoc test. $^{**}P<0.01$ and $^{***}P<0.001$

is highly expressed in chondrocytes, involved in endochondral ossification and cartilage maturation [26]. The N-terminal structural divergence leads to distinct target gene specificity. Type II Runx2 dominates osteogenesis, while type-I Runx2 may suppress certain osteogenic genes. However, the antibodies used in previous studies to identify Runx2 proteins were generated against regions common to both type-I and type-II isoforms [27, 28]. There is no antibody currently available to distinguish type-I and type-II Runx2 proteins [25]. That explains why the expression of Runx2 in bone is contradictory [29]. In the study of Park et al. [14], they reported the upregulated Runx2 expression following OB treatment. Considering they detected Runx2 expression in an osteoblast cell line MC3T3-E1, we inferred that the type-II Runx2 was analyzed. In our study, we detected Runx2 in chondrocytes; so, the type-I Runx2 was analyzed. That's might be why the opposite expression of Runx2 was observed between our studies. 2) Herbal medicines induce complex regulation network in different cell types. In the study of Park et al. [14], they demonstrated OB to upregulate Runx2 expression via targeting GSK3β. In our study, we demonstrated that OB exhibited the opposite regulation Runx2 expression via targeting HDACs. The different regulation on the targets might be result in the different regulation on the downstream genes. That might be another reason of the contradiction for Runx2 expression. Our hypothesis should be further confirmed in the following using the antibodies specific against type-I or type-II isoforms.

Recently, increasing attention has focused on anti-inflammatory therapy as the most promising approach for the OA treatment [30, 31]. Chondrocytes are found in various cartilage tissue types and are responsible

for the growth and maintenance of cartilage tissues. Imbalanced inflammation can activate chondrocytes and increase the secretion of pro-inflammatory cytokines [32]. Moreover, excessive inflammation may induce degradation of the ECM of cartilage by promoting collagenase and aggrecanase expression [33, 34]. IL-18 is spontaneously released from OA chondrocytes and participate in inflammation and destructive alterations of ECM via induction of TNF-α [35]. Previous studies indicated that OB is a potential agent for inhibiting inflammation in multiple diseases, including chronic inflammation-associated colorectal cancer [36], liver fibrosis [37], acute lung injury [38], and ulcerative colitis [39]. In this study, the anti-inflammatory functions of OB were observed in animal and cell models of OA, indicating the benefit of using OB as a therapeutic agent for OA and other inflammatory diseases.

HDACs are a class of enzymes that regulate gene expression by removing acetyl groups from histones. They work in concert with histone acetyltransferases (HATs) to maintain the balance of histone acetylation, thereby influencing chromatin structure and gene transcription [40]. HDACs are involved in the regulation of cartilage lesions and cartilage degeneration during OA progression. HDAC inhibitors are considered promising therapeutic interventions for OA [17, 41, 42]. Chen et al. [43] demonstrated that trichostatin A acts as an HDAC inhibitor and attenuates cartilage degradation in rabbit OA models. Zhong et al. [44] reported that vorinostat is an HDAC inhibitor that exhibits chondroprotective activity during OA progression. In this study, bioinformatic analyses predicted OB might be a pan-HDAC inhibitor. In vitro studies suggested that HDAC1 is a target for OB and that OB binding inhibits its HDAC1 stability. Furthermore, OB docking with HDAC1 limits the activation of p38MAPK signaling, which significantly participates in chondrocyte death, inflammation, and cartilage ECM degradation [45]. However, the effects of OB on other HDACs, including HDAC2, 3, 4, and 9 should be further studied in the following. In addition, multiple signaling pathways, including NF-κB, ERK, and JNK [17, 41], are also well-known to be involved in the regulating effects of HDAC in treating OA; further investigations focused on these signaling pathways will expand our understanding of the mechanisms of the anti-OA action of OB.

In conclusion, we determined the chondroprotective role of OB in OA development. OB inhibits HDAC1 protein stability and limits p38MAPK activation to control OA progression. This study provides a promising therapeutic strategy for the treatment of OA.

Acknowledgements
None.

Authors' contributions
Y G: designed the study and performed the research; K W, C S and Yang G: performed the research, analyzed data; DQ K: analyzed data and wrote the paper.

Funding
No funding.

Data availability
No datasets were generated or analysed during the current study.

Declarations

Ethics approval and consent to participate
The Ethics Committee of The Second Affiliated Hospital of Shandong First Medical University approved the research. The animal experimental was performed in accordance with ARRIVE guidelines.

Consent for publication
None.

Competing interests
The authors declare no competing interests.

Author details
[1]Department of Orthopaedic Surgery, The Second Affiliated Hospital of Shandong First Medical University, No. 366, Taishan Street, Taishan District, Tai'an City, Shandong Province, China. [2]Rehabilitation Department, Taishan Vocational College of Nursing, Tai'an City, Shandong Province, China.

Received: 26 February 2025 Accepted: 10 April 2025
Published online: 03 May 2025

References

1. Minnig MCC, Golightly YM, Nelson AE. Epidemiology of osteoarthritis: literature update 2022–2023. Curr Opin Rheumatol. 2024;36(2):108–12.
2. GBD 2021 Gout Collaborators. Global, regional, and national burden of gout, 1990–2020, and projections to 2050: a systematic analysis of the Global Burden of Disease Study 2021. Lancet Rheumatol. 2024;6(8):e507-e517.
3. Hawker GA, King LK. The burden of osteoarthritis in older adults. Clin Geriatr Med. 2022;38(2):181–92.
4. Yao Q, Wu X, Tao C, Gong W, Chen M, Qu M, Zhong Y, He T, Chen S, Xiao G. Osteoarthritis: pathogenic signaling pathways and therapeutic targets. Signal Transduct Target Ther. 2023;8(1):56.
5. Sanchez-Lopez E, Coras R, Torres A, Lane NE, Guma M. Synovial inflammation in osteoarthritis progression. Nat Rev Rheumatol. 2022;18(5):258–75.
6. Molnar V, Matišić V, Kodvanj I, Bjelica R, Jeleč Ž, Hudetz D, Rod E, Čukelj F, Vrdoljak T, Vidović D, et al. Cytokines and chemokines involved in osteoarthritis pathogenesis. Int J Mol Sci. 2021;22(17):9208.
7. Troeberg L, Nagase H. Proteases involved in cartilage matrix degradation in osteoarthritis. Biochim Biophys Acta. 2012;1824(1):133–45.
8. Hodgkinson T, Kelly DC, Curtin CM, O'Brien FJ. Mechanosignalling in cartilage: an emerging target for the treatment of osteoarthritis. Nat Rev Rheumatol. 2022;18(2):67–84.
9. Knights AJ, Redding SJ, Maerz T. Inflammation in osteoarthritis: the latest progress and ongoing challenges. Curr Opin Rheumatol. 2023;35(2):128–34.
10 Zhou Y, Gu J, Li J, Zhang H, Wang M, Li Y, Wang T, Wang J, Shi R. Obacunone, a promising phytochemical triterpenoid: research progress on its pharmacological activity and mechanism. Molecules. 2024;29(8):1791.
11. Chen Y, Liu H, Han R, Lin J, Yang J, Guo M, Yang Z, Song L. Analyzing how SiMiao Wan regulates ferroptosis to prevent RA-ILD using metabolomics and cyberpharmacology. Phytomedicine. 2024;133:155912.
12. He J, Zheng L, Li X, Huang F, Hu S, Chen L, Jiang M, Lin X, Jiang H, Zeng Y, et al. Obacunone targets macrophage migration inhibitory factor (MIF) to

impede osteoclastogenesis and alleviate ovariectomy-induced bone loss. J Adv Res. 2023;53:235–48.
13. Hu H, Wang X, Huang Y, He B, Zhu J, Sun K, Deng C, Guo Y, Hao D, Jian B. Obacunone inhibits RANKL/M-CSF-mediated osteoclastogenesis by suppressing integrin- FAK-Src signaling. Cytokine. 2023;164:156134.
14. Park KR, Kim S, Cho M, Yun HM. Limonoid triterpene, obacunone increases runt-related transcription factor 2 to promote osteoblast differentiation and function. Int J Mol Sci. 2021;22(5):2483.
15. Kamekura S, Hoshi K, Shimoaka T, Chung U, Chikuda H, Yamada T, Uchida M, Ogata N, Seichi A, Nakamura K, et al. Osteoarthritis development in novel experimental mouse models induced by knee joint instability. Osteoarthritis Cartilage. 2005;13(7):632–41.
16. Glasson SS, Chambers MG, Van Den Berg WB, Little CB. The OARSI histopathology initiative - recommendations for histological assessments of osteoarthritis in the mouse. Osteoarthritis Cartilage. 2010;18(Suppl 3):S17-23.
17. Khan NM, Haqqi TM. Epigenetics in osteoarthritis: potential of HDAC inhibitors as therapeutics. Pharmacol Res. 2018;128:73–9.
18. Hong S, Derfoul A, Pereira-Mouries L, Hall DJ. A novel domain in histone deacetylase 1 and 2 mediates repression of cartilage-specific genes in human chondrocytes. Faseb J. 2009;23(10):3539–52.
19. Abramoff B, Caldera FE. Osteoarthritis: pathology, diagnosis, and treatment options. Med Clin North Am. 2020;104(2):293–311.
20. Sugimoto K, Iizawa T, Harada H, Yamada K, Katsumata M, Takahashi M. Cartilage degradation independent of MMP/aggrecanases. Osteoarthritis Cartilage. 2004;12(12):1006–14.
21. Catheline SE, Hoak D, Chang M, Ketz JP, Hilton MJ, Zuscik MJ, Jonason JH. Chondrocyte-specific RUNX2 overexpression accelerates post-traumatic osteoarthritis progression in adult mice. J Bone Miner Res. 2019;34(9):1676–89.
22 Ashruf OS, Ansari MY. Natural compounds: potential therapeutics for the inhibition of cartilage matrix degradation in osteoarthritis. Life (Basel). 2022;13(1):102.
23. Horcajada MN, Beaumont M, Sauvageot N, Poquet L, Saboundjian M, Costes B, Verdonk P, Brands G, Brasseur J, Urbin-Choffray D, et al. An oleuropein-based dietary supplement may improve joint functional capacity in older people with high knee joint pain: findings from a multicentre-RCT and post hoc analysis. Ther Adv Musculoskelet Dis. 2022;14:1759720x211070205.
24. Wang J, Ma J, Gu JH, Wang FY, Shang XS, Tao HR, Wang X. Regulation of type II collagen, matrix metalloproteinase-13 and cell proliferation by interleukin-1β is mediated by curcumin via inhibition of NF-κB signaling in rat chondrocytes. Mol Med Rep. 2017;16(2):1837–45.
25. Sudhakar S, Katz MS, Elango N. Analysis of type-I and type-II RUNX2 protein expression in osteoblasts. Biochem Biophys Res Commun. 2001;286(1):74–9.
26. Ducy P, Zhang R, Geoffroy V, Ridall AL, Karsenty G. Osf2/Cbfa1: a transcriptional activator of osteoblast differentiation. Cell. 1997;89(5):747–54.
27. Manzotti G, Torricelli F, Donati B, Sancisi V, Gugnoni M, Ciarrocchi A. HDACs control RUNX2 expression in cancer cells through redundant and cell context-dependent mechanisms. J Exp Clin Cancer Res. 2019;38(1):346.
28. Qin X, Jiang Q, Komori H, Sakane C, Fukuyama R, Matsuo Y, Ito K, Miyazaki T, Komori T. Runt-related transcription factor-2 (Runx2) is required for bone matrix protein gene expression in committed osteoblasts in mice. J Bone Miner Res. 2021;36(10):2081–95.
29. Komori T. Runx2, an inducer of osteoblast and chondrocyte differentiation. Histochem Cell Biol. 2018;149(4):313–23.
30. Conaghan PG, Cook AD, Hamilton JA, Tak PP. Therapeutic options for targeting inflammatory osteoarthritis pain. Nat Rev Rheumatol. 2019;15(6):355–63.
31. Di Francesco M, Fragassi A, Pannuzzo M, Ferreira M, Brahmachari S, Decuzzi P. Management of osteoarthritis: From drug molecules to nano/micromedicines. Wiley Interdiscip Rev Nanomed Nanobiotechnol. 2022;14(3):e1780.
32. Zheng L, Zhang Z, Sheng P, Mobasheri A. The role of metabolism in chondrocyte dysfunction and the progression of osteoarthritis. Ageing Res Rev. 2021;66:101249.
33. Ansari MY, Ahmad N, Haqqi TM. Oxidative stress and inflammation in osteoarthritis pathogenesis: role of polyphenols. Biomed Pharmacother. 2020;129:110452.
34. Guo Q, Chen X, Chen J, Zheng G, Xie C, Wu H, Miao Z, Lin Y, Wang X, Gao W, et al. STING promotes senescence, apoptosis, and extracellular matrix degradation in osteoarthritis via the NF-κB signaling pathway. Cell Death Dis. 2021;12(1):13.
35. Matsui K, Tsutsui H, Nakanishi K. Pathophysiological roles for IL-18 in inflammatory arthritis. Expert Opin Ther Targets. 2003;7(6):701–24.
36. Luo X, Yu Z, Yue B, Ren J, Zhang J, Mani S, Wang Z, Dou W. Obacunone reduces inflammatory signalling and tumour occurrence in mice with chronic inflammation-induced colorectal cancer. Pharm Biol. 2020;58(1):886–97.
37. Han Y, Luo L, Li H, Zhang L, Yan Y, Fang M, Yu J, Gao X, Liu Y, Huang C, et al. Nomilin and its analogue obacunone alleviate NASH and hepatic fibrosis in mice via enhancing antioxidant and anti-inflammation capacity. BioFactors. 2023;49(6):1189–204.
38. Chen Y, Peng M, Li W, Zhao M, Cao X, Li C, Zhang H, Yang M, Liang L, Yue Y, et al. Inhibition of inflammasome activation via sphingolipid pathway in acute lung injury by Huanglian Jiedu decoction: an integrative pharmacology approach. Phytomedicine. 2022;107:154469.
39. Luo X, Yue B, Yu Z, Ren Y, Zhang J, Ren J, Wang Z, Dou W. Obacunone protects against ulcerative colitis in mice by modulating gut microbiota, attenuating TLR4/NF-κB signaling cascades, and improving disrupted epithelial barriers. Front Microbiol. 2020;11:497.
40. Shanmugam G, Rakshit S, Sarkar K. HDAC inhibitors: targets for tumor therapy, immune modulation and lung diseases. Transl Oncol. 2022;16:101312.
41. Zhang H, Ji L, Yang Y, Zhang X, Gang Y, Bai L. The role of HDACs and HDACi in cartilage and osteoarthritis. Front Cell Dev Biol. 2020;8:560117.
42. Carpio LR, Westendorf JJ. Histone deacetylases in cartilage homeostasis and osteoarthritis. Curr Rheumatol Rep. 2016;18(8):52.
43. Chen WP, Bao JP, Hu PF, Feng J, Wu LD. Alleviation of osteoarthritis by Trichostatin A, a histone deacetylase inhibitor, in experimental osteoarthritis. Mol Biol Rep. 2010;37(8):3967–72.
44. Zhong HM, Ding QH, Chen WP, Luo RB. Vorinostat, a HDAC inhibitor, showed anti-osteoarthritic activities through inhibition of iNOS and MMP expression, p38 and ERK phosphorylation and blocking NF-κB nuclear translocation. Int Immunopharmacol. 2013;17(2):329–35.
45. Li Z, Dai A, Yang M, Chen S, Deng Z, Li L. p38MAPK signaling pathway in osteoarthritis: pathological and therapeutic aspects. J Inflamm Res. 2022;15:723–34.

Publisher's Note